Robotica (2016) volume 34, pp. 859–875. © Cambridge University Press 2014
doi:10.1017/S026357471400191X

Transparent four-channel bilateral control architecture using modified wave variable controllers under time delays

Da Sun*, Fazel Naghdy and Haiping Du

School of Electrical, Computer and Telecommunication Engineering, Faculty of Engineering and Information Sciences, University of Wollongong, Wollongong NSW 2522, Australia.
E-mails: fazel@uow.edu.au, hdu@uow.edu.au

(Accepted June 19, 2014. First published online: July 17, 2014)

SUMMARY
Stability and transparency are two critical indices of bilateral teleoperation systems. The wave variable method is a conservative approach to robustly guarantee system passivity under arbitrary constant time delays. However, the wave-variable-based reflection is an intrinsic problem in this method because it can significantly degrade system transparency and disorient the operator's perception of the remote environment. In order to enhance both the transparency and the stability of bilateral teleoperation systems in the presence of large time delays, a new four-channel (4-CH) architecture is proposed which applies two modified wave-transformation controllers to reduce wave-based reflections. Transparency and stability of the proposed system are analyzed and the improvement in these when using this method is measured experimentally. Results clearly demonstrate that the proposed method can produce high transparency and stability even in the presence of large time delays.

KEYWORDS: Bilateral teleoperation; Wave variable method; Wave-based reflection; 4-CH architecture; Passivity; Transparency; Time delay; Position drift.

1. Introduction

Teleoperation allows a human operator to interact remotely with the environment, and human sensing, decision making, and operation ability are extended far beyond the direct physical connection. In a bilateral teleoperation system, in which information flows in both directions between the operator and the environment, the contact force information is fed back from the slave to the master in order to provide a realistic experience for the human operator. The quality of such a system is primarily measured through two critical indices: stability and transparency. The system stability means the whole closed-loop system is stable no matter how the human operator and the remote environment change. Transparency indicates that the technical medium between the operator and the environment is not felt, i.e., the dynamics of master and slave are canceled out.[1] Since force feedback may cause instability, achieving a trade-off between stability and transparency is a challenge in bilateral teleoperation systems.[2] In addition, system stability is quite sensitive to time delays. Even a small time delay can seriously threaten the system stability.

Numerous methods have been proposed to deal with the trade-off between stability and transparency under time delays.[3–7] Among them, the wave variable method is identified as an effective way to robustly guarantee stability of a delay-based teleoperation system which is based on wave variables instead of conventional power variables, i.e., velocity and force, during signal transmission. Based on passivity, the framework of wave variables for designing and analyzing force-reflecting teleoperators seeks to avoid energy generation in the system and leads to efficient implementations without prior knowledge of the time delay. However, as a conservative method on passivity of delay-based system, it has one major disadvantage known as wave-based reflection. This phenomenon can

* Corresponding author. E-mail: ds744@uowmail.edu.au

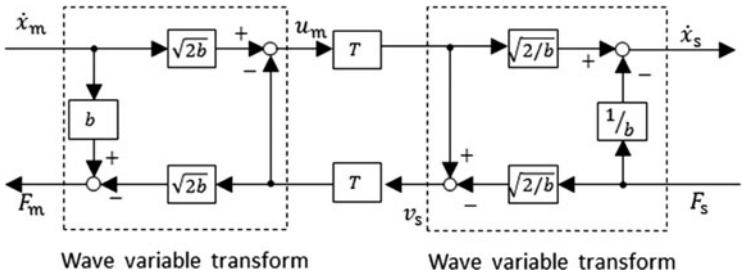

Fig. 1. Standard wave transformation controller.

greatly hamper transparency since it makes the teleoperation system produce oscillations, especially under large time delays.

Many approaches have been proposed to enhance the performance of the wave-variable-based system. Yokokohji *et al.* design a compensator to minimize the system's performance degradation using the wave integral method.[8,9] Munir *et al.* propose the wave prediction approach using the Kalman filter to model the communication delays and enhance the position tracking performance in free space.[10,11] Ye *et al*. design two new architectures based on wave controllers with correction terms to enhance force-tracking and trajectory-tracking performances.[12,13] Tian *et al*. explore the relationship between the wave variable and the 4-CH architecture in the frequency domain.[14] By applying the wave controllers, Aziminejad *et al*. transform four communication channels of the 4-CH architecture into two channels to transmit the wave signals.[15] Yalcin *et al*. use an acceleration controller to combine the wave controllers with the 4-CH architecture.[16] Since the wave-variable-based reflection problem is not thoroughly addressed in these studies, achieving an optimal trade-off between stability and transparency in the time-delayed wave-variable-based system still remains a big problem.

In this paper, a new 4-CH architecture is proposed to achieve ideal delay-based transparency in which two modified wave transformation controllers are applied to reduce the wave-based reflections and simultaneously guarantee the passivity of the communication channels in the presence of large time delays. The conditions required to realize an optimal trade-off between stability and transparency are also analyzed.

The remainder of this paper is structured as follows: Section 2 introduces the background on the wave variable method and wave-based reflection and Section 3 describes the proposed scheme. In Section 3, the delay-based stability and the conditions for realizing transparency of the proposed system are also analyzed. Section 4 presents the experimental results and compares the proposed system with previous work. Some conclusions are drawn in Section 5.

2. Background

2.1. Passivity and wave variables

A standard wave transformation controller is illustrated in Fig. 1. As shown in Fig. 1 and the related Eq. (1),[21] the wave-encoding mechanism defines a complementary pair of wave variables (the forward wave variable u_m and the returning wave variable v_s) in terms of standard power signals (velocity $\dot{x}_{m/s}$ and force $F_{m/s}$) in this system. The notations m and s refer to "master" and "slave," respectively.

$$u_m = \frac{b\dot{x}_m + F_m}{\sqrt{2b}}, \; v_s = \frac{b\dot{x}_s - F_s}{\sqrt{2b}}, \tag{1}$$

where b is the wave characteristic impedance. The power flow is decoupled into the forward flow and the feedback flow:

$$P = \dot{x}^T F = \frac{1}{2}u^T u - \frac{1}{2}v^T v. \tag{2}$$

Control system passivity is achieved if the sum of the initial stored energy and the energy injected into the system is larger than, or equal to, the energy output.[17] A wave-variable-based teleoperation

https://doi.org/10.1017/S026357471400191X Published online by Cambridge University Press

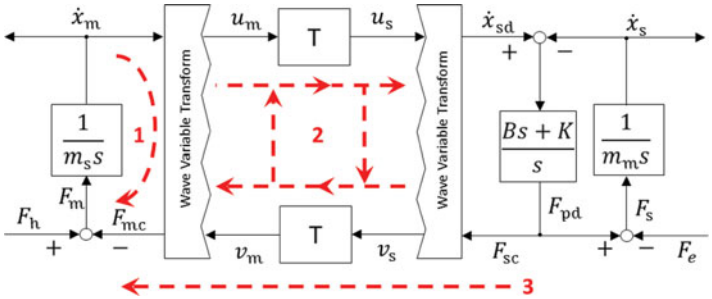

Fig. 2. Wave-based reflection due to impedance junctions.

system is passive when it satisfies the following condition:

$$\int_0^t \frac{1}{2} v^T v \leq \int_0^t \frac{1}{2} u^T u + E_{\text{store}}(0), \quad \forall t \geq 0, \tag{3}$$

where $E_{\text{store}}(0)$ denotes the initial energy stored in the system.

Based on the scattering theory, for a linear time invariant (LTI) two-port network with force vector $F = [F_m F_s]^T$ and velocity vector $\dot{x} = [\dot{x}_m \dot{x}_s]^T$, the scattering matrix can be expressed as

$$F - \dot{x} = S(s)(F + \dot{x}), \tag{4}$$

where parameter s ($s = j\omega$) is the Laplace operator. The necessary and sufficient condition for the passivity of a wave-based system is when the norm of the scattering matrix $S(s)$ is no more than 1. That is,$S \leq 1$.[3] This also enables absolute stability in a general two-port network.

2.2. Wave-based reflection

The phenomenon of wave reflection, which is due to imperfectly matched junction impedance, was first observed by Niemeyer and Slotine.[18] The standard wave-variable-based system shown in Fig. 2 consists of three independent channels: the master's direct feedback (dotted line 1), the wave-variable-based reflections (dotted line 2), and the slave's force feedback to the master (dotted line 3). In channel 1, the master velocity signals directly return as the damping $b\dot{x}_m$, which can be treated as a simple damper. A certain amount of damping produced in channel 1 enhances the system stability by sacrificing transparency. Channel 3 feeds force information back to the operator from the remote slave side. The phenomenon of wave-variable-based reflection occurs in channel 2. Rewriting (1),

$$u_m = -v_m + \sqrt{2b}\dot{x}_m, \tag{5}$$

$$v_s = -u_s + \sqrt{2/b} F_s. \tag{6}$$

Based on (5) and (6), each incoming wave variable v_m and u_s is reflected and returned as the outgoing wave variable u_m and v_s, respectively. Wave-variable-based reflection lasts several cycles in the communication channels and then gradually disappears. This phenomenon can easily generate unpredictable interference and disturbances which may make the system unstable.

The velocity and force tracking of the standard wave-variable-based system in Fig. 2 are written as follows:

$$\dot{x}_{sd}(s) = \dot{x}_m(s) e^{-sT} - \frac{1}{b}\left[F_{sc}(s) - F_{mc}(s) e^{-sT}\right], \tag{7}$$

$$F_{mc}(s) = F_{sc}(s) e^{-sT} + b\left[\dot{x}_m(s) - \dot{x}_{sd}(s) e^{-sT}\right], \tag{8}$$

where $\dot{x}_{sd}$, F_{mc}, and F_{sc} denote desired velocity command from the slave manipulator, master control force, and slave control force, respectively. The wave-variable-based reflections in channel 2

https://doi.org/10.1017/S026357471400191X Published online by Cambridge University Press

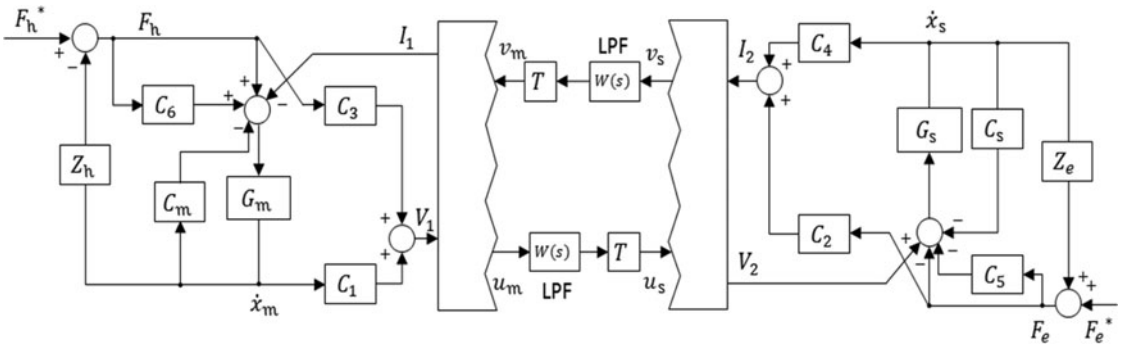

Fig. 3. 4-CH architecture applying wave transmission.[15]

adversely influence the transmitted force and velocity signals so that $F_{sc}(s)$ and $\dot{x}_m(s)$ are not equal to $F_{mc}(s)e^{-sT}$ and $\dot{x}_{sd}(s)e^{-sT}$, respectively. Hence, the bias terms $-\frac{1}{b}[F_{sc}(s) - F_{mc}(s)e^{-sT}]$ in (7) and $b[\dot{x}_m(s) - \dot{x}_{sd}(s)e^{-sT}]$ in (8) can degrade the large delay-based system transparency, especially during the transient state of the system.

Under ideal conditions, when the teleoperation system impedance is perfectly matched, the feed-forward wave variable u_m and the feedback wave variable v_s only contain velocity information and force information, respectively:[19,20]

$$u_m(s) = \frac{b\dot{x}_m(s)}{\sqrt{2b}},\ v_s(s) = \frac{F_{sc}(s)}{\sqrt{2b}} \tag{9}$$

When the impedance is perfectly matched, u_m and v_s will not be influenced by the input wave variables u_s and v_m. Hence, the wave-variable-based reflections can be avoided. The remaining problem is that the added impedance matching terms can significantly degrade the velocity and force tracking performance. Based on Fig. 3, $\dot{x}_s$ and F_m are expressed as:

$$\dot{x}_{sd}(s) = \frac{b\dot{x}_m(s)\,e^{-sT} - F_s(s)}{2b}, \tag{10}$$

$$F_{mc}(s) = \frac{b\dot{x}_m(s) - F_{sc}(s)e^{-sT}}{2}. \tag{11}$$

Based on (10) and (11), if F_s decays to zero, $\dot{x}_s$ equals to $\frac{\dot{x}_m}{2}$. On the other hand, if the master manipulator moves slowly and finally the master velocity decays to zero, F_m will converge to $-\frac{F_s}{2}$. In this situation, the velocity, and the force tracking performance will become much poorer.

Slave impedance matching is a method to deal with the wave-variable-based reflections by adding predetermined damping elements.[18] However, the predetermined damping elements are not able to address the unknown impedance changes of the operator and the environment and this means that the wave-variable-based reflections are reinstated.

Another method to handle unknown changes of operator and environmental impedance is wave filtering through adding a low-pass filter to the feed-forward path.[18] Combined with impedance matching, either the wave-variable-based reflection in free space or the wave reflection brought about by the operator or the remote environment can, to some extent, be reduced. Nevertheless, this approach has an obvious disadvantage: the low-pass filters in the feed-forward channel can significantly restrict the bandwidth of the communication channel.

A new scheme for reducing wave reflection is proposed in ref. [21]. The outgoing wave variables of this scheme are expressed as:

$$u_m(s) = \frac{b\dot{x}_m(s) + F_{sc}(s)\,e^{-sT}}{\sqrt{2b}}, \tag{12}$$

$$v_s(s) = \frac{F_{sc}(s)}{\sqrt{2b}}. \tag{13}$$

https://doi.org/10.1017/S026357471400191X Published online by Cambridge University Press

Unlike (1), the outgoing slave wave variable v_s in (13), which contains no velocity information, retains no information from the incoming wave variable u_s. Therefore, the wave-variable-based reflections can be prevented. Based on (12) and (13), the velocity and force tracking equations are written as:

$$b\dot{x}_{sd}(s) = b\dot{x}_m(s)\,e^{-sT} + \left[F_{sc}(s)\,e^{-2sT} - F_{sc}(s)\right], \tag{14}$$

$$F_{mc}(s) = b\dot{x}_m(s) + F_{sc}(s)\,e^{-sT}. \tag{15}$$

According to (14), precise velocity tracking can be achieved under constant time delay or delay with slowly time varying conditions. Under the completely hard environment contact condition (no movement of the master manipulator), (15) indicates that accurate force reflection can also be achieved. However, if the master manipulator still has velocity during contact with the environment, this system will generate inaccurate force tracking due to the bias term $b\dot{x}_m(s)$ in (15). The inaccurate force tracking can also adversely affect the position tracking when contacting the environment so that large position drift will occur in this architecture.

2.3. 4-CH architecture with wave variable controller

It has been demonstrated that the 4-CH architecture with the extra "degrees of freedom" (control parameters) is the best teleoperation system from transparency point of view when the communication channels have no time delay.[5,22] However, the 4-CH system suffers from stability degradation in the presence of time delays.[15] In order to guarantee the stability of the delay-based channels, Aziminejad *et al.*[15] extend the wave transmission to the extended Lawrence 4-CH architecture illustrated in refs. [23] and [24]. To combine the wave transmission with the extended Lawrence architecture, the communication channel part of the system is segregated as a two-port network, as shown in Fig. 3.

In Fig. 3, the non-physical input and output efforts and flow of the communication channel are expressed as:

$$V_1 = C_3F_h + C_1\dot{x}_m,\; V_2 = F_e(1 + C_5) + \dot{x}_s(M_s s + C_s), \tag{16}$$

$$I_1 = F_h(1 + C_6) - \dot{x}_m(M_m s + C_m),\; I_2 = C_2F_e + C_4\dot{x}_s, \tag{17}$$

where controllers C_2, C_3, C_5, and C_6 are force controllers, while C_1, C_4, C_s, and C_m are velocity controllers.

In this scheme, the wave variables can be written as

$$u = \frac{bI + V}{\sqrt{2b}},\; v = \frac{bI - V}{\sqrt{2b}}. \tag{18}$$

By extending the wave-variable method into the 4-CH architecture, the trade-off between the stability and the transparency of the bilateral teleoperation is better than that in the conventional wave-variable-based system. Since the application of the extended Laurence architecture allows for the transmission of the position signals, the position drift problem of the wave-variable-based system can be somewhat reduced. In order to overcome the oscillations caused by the wave-variable-based reflection and guarantee the delay-based stability, Aziminejad *et al.* continue to apply the wave-filtering approach where the cutoff frequency f_{cut} of the first-order low-pass filters $W(s) = \frac{2\pi f_{cut}}{(s+2\pi f_{cut})}$ located at the transmission paths must be set as a small value. Therefore, the bandwidth of the communication channels is seriously restricted. Moreover, even applying extra control parameters of the 4-CH architecture, the bias terms of the wave-variable-based system in (7) and (8) are still not thoroughly compensated for. Combining (16) and (17) into (18),

$$\begin{aligned}(1 + C_5 + bC_2)\,F_e &= (C_3 + b + bC_6)\,F_h \times e^{-sT}W \\ &+ [(M_s s + C_s + bC_4)\,\dot{x}_s - (C_1 - bM_m s - bC_m)\,\dot{x}_m \times e^{-sT}W],\end{aligned} \tag{19}$$

https://doi.org/10.1017/S026357471400191X Published online by Cambridge University Press

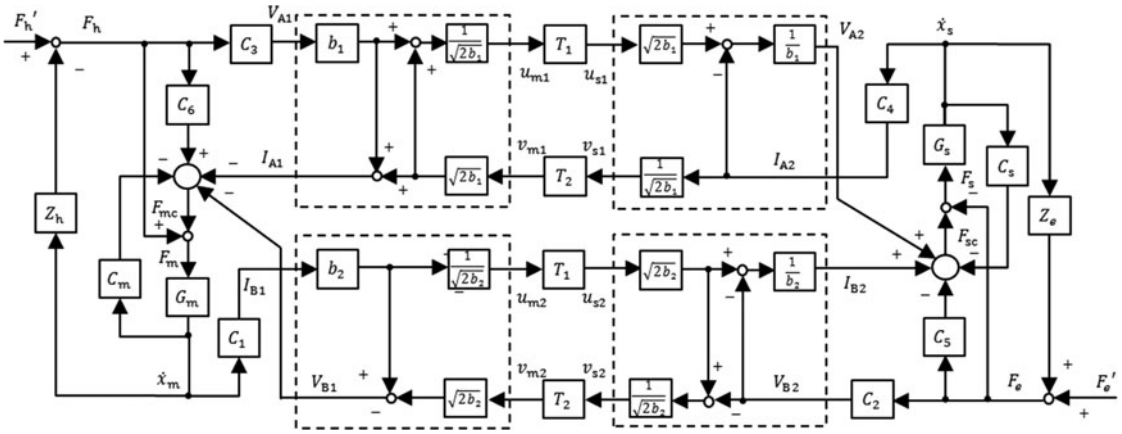

Fig. 4. Proposed 4-CH architecture with modified wave controllers.

$$(bM_{\mathrm{m}}s + bC_{\mathrm{m}} + C_1)\,\dot{x}_{\mathrm{m}} = (M_{\mathrm{s}}s + C_{\mathrm{s}} - bC_4)\,\dot{x}_{\mathrm{s}} \times e^{-sT}W + \left[(b + bC_6 - C_3)\,F_{\mathrm{h}} \times e^{-sT}W - (bC_2 - 1 - C_5)\,F_e\right]. \tag{20}$$

Based on (19) and (20), both the velocity and force tracking performance of the system in ref. [15] are degraded by the bias terms $[(M_{\mathrm{s}}s + C_{\mathrm{s}} + bC_4)\dot{x}_{\mathrm{s}} - (C_1 - bM_{\mathrm{m}}s - bC_{\mathrm{m}})\dot{x}_{\mathrm{m}} \times e^{-sT}W]$ and $[(b + bC_6 - C_3)F_{\mathrm{h}} \times e^{-sT}W - (bC_2 - 1 - C_5)F_e]$ during the signal transmission between master and slave. This means that even applying extra control parameters, it is impossible for the system in ref. [15] to achieve ideal transparency in the presence of large time delays.

3. Proposed Method

3.1. Design

In this work, a new 4-CH architecture with modified wave variable controllers is proposed (see Fig. 4). The goal of this architecture is to reduce wave-based reflection, to enhance system transparency and simultaneously guarantee system stability in the presence of time delays.

In Fig. 4, two modified wave transformation schemes for reducing wave-based reflection are applied to guarantee the stability of the delay-based communication channels. A wave controller with characteristic impedance b_1 is used to encode the controlled human operator's force V_{A1} and the controlled slave velocity I_{A2}. The wave variables in this wave controller are defined as:

$$u_{\mathrm{m1}}(s) = \frac{b_1 V_{A1}(s) + I_{A2}(s)\,e^{-sT_1}}{\sqrt{2b_1}},$$
$$u_{\mathrm{s1}}(s) = \frac{b_1 V_{A2}(s) + I_{A2}(s)}{\sqrt{2b_1}}, \tag{21}$$
$$v_{\mathrm{m1}} = \frac{I_{A2}(s)e^{-sT_2}}{\sqrt{2b_1}},\ v_{\mathrm{s1}}(s) = \frac{I_{A2}(s)}{\sqrt{2b_1}}. \tag{22}$$

As in (12) and (13), since v_{s1} in (22) no longer contains the force information so that the slave's outgoing wave variable v_{s1} does not retain any information from the incoming wave variable u_{s1}. Therefore the wave-variable-based reflections in the first two channels can be eliminated.

The controlled environmental force V_{B2} and the controlled master velocity I_{B1} are encoded by the wave controller with the characteristic impedance b_2. The wave variables in this wave controller are

https://doi.org/10.1017/S026357471400191X Published online by Cambridge University Press

defined as:

$$u_{\mathrm{m}2}(s) = \frac{b_2 I_{B1}(s)}{\sqrt{2b_2}}, u_{\mathrm{s}2}(s) = \frac{b_2 I_{B1}(s) e^{-sT_1}}{\sqrt{2b_2}}, \tag{23}$$

$$v_{\mathrm{m}2}(s) = \frac{b_2 I_{B1}(s) - V_{B1}(s)}{\sqrt{2b_2}},$$

$$v_{\mathrm{s}2}(s) = \frac{b_2 I_{B1}(s) e^{-sT_1} - V_{B2}(s)}{\sqrt{2b_2}}. \tag{24}$$

As shown in (23), the feed-forward wave variables $u_{\mathrm{m}2}$ and $u_{\mathrm{s}2}$ do not contain any force information to the extent that any information regarding the feedback wave variable $v_{\mathrm{m}2}$ is no longer included in the outgoing master wave variable $u_{\mathrm{m}2}$. Therefore, since the proposed wave transformation controller at the master side decouples the velocity and force information, circulating wave reflections in the last two channels can be prevented.

The wave transmissions between the master and slave sides in this system are expressed as (25):

$$\begin{cases} u_{\mathrm{m}1}(s) e^{-sT_1} = u_{s1}(s) \\ v_{\mathrm{m}1}(s) = v_{s1}(s) e^{-sT_2} \\ u_{\mathrm{m}2}(s) e^{-sT_3} = u_{s2}(s) \\ v_{\mathrm{m}2}(s) = v_{s2}(s) e^{-sT_4} \end{cases}. \tag{25}$$

Substituting (21)–(24) into (25), the controlled force and velocity transmission in the proposed system can be expressed by:

$$V_{A2}(s) = V_{A1}(s) e^{-sT_1} + \frac{1}{b_1}\left[I_{A2}(s) e^{-s(T_1+T_2)} - I_{A2}(s)\right], \tag{26}$$

$$I_{A1}(s) = b_1 V_{A1}(s) + I_{A2}(s) e^{-sT_2}, \tag{27}$$

$$V_{B1}(s) = V_{B2}(s) e^{-sT_2} + b_2\left[I_{B1}(s) - I_{B1}(s) e^{-s(T_1+T_2)}\right], \tag{28}$$

$$I_{B2}(s) = I_{B1}(s) e^{-sT_1} - \frac{1}{b_2} V_{B2}(s). \tag{29}$$

According to (26) and (28), since the effect of the wave-variable-based reflections is cancelled in the feed-forward and feedback controlled velocity transmission channels, the bias term $\frac{1}{b_1}[I_{A2}(s)e^{-s(T_1+T_2)} - I_{A2}(s)]$ and $b_2[I_{B1}(s) - I_{B1}(s)e^{-s(T_1+T_2)}]$ is near zero. Under constant time delay or time delay with slow variation, (26) and (28) show a highly accurate force tracking performance. This advantage allows the proposed teleoperator to handle different kinds of unknown environments and provides the operator with accurate perception of the remote environment. The major disadvantage of the two modified wave transformation controllers (shown in (27) and (29)) is that the bias terms $b_1 V_{A1}(s)$ and $-\frac{1}{b_2} V_{B2}(s)$ can degrade the trajectory tracking performance especially during the environmental contact with a large force values of V_{A1} and $V_{B2}(s)$. Therefore, position drift can occur if using only one of the two wave transformation controllers in a 2-CH channel architecture. However, the bias terms $b_1 V_{A1}(s)$ and $-\frac{1}{b_2} V_{B2}(s)$ cannot be cancelled since they are treated as the dampers to guarantee the delay-based system stability. Accordingly, the controllers in 4-CH architectures are applied to compensate for the bias terms and enhance transparency.

On the master and slave sides, $G_{\mathrm{m}} = \frac{1}{M_{\mathrm{m}} s}$ and $G_{\mathrm{s}} = \frac{1}{M_{\mathrm{s}} s}$ are the transfer functions of the master and slave manipulators where M_{m} and M_{s} are the masses of the slave and master, respectively. C_2, C_3, C_5, and C_6 are the force control gains and C_1, C_4, C_{s} and C_{m} are the velocity controllers. The dynamics of the slave and the master manipulators can be expressed as

$$(G_{\mathrm{m}}^{-1} + C_{\mathrm{m}})\dot{x}_{\mathrm{m}}(s) = (1 + C_6) F_{\mathrm{h}}(s) - I_{A1}(s) - V_{B1}(s), \tag{30}$$

$$(G_{\mathrm{s}}^{-1} + C_{\mathrm{s}})\dot{x}_{\mathrm{s}}(s) = I_{B2}(s) + V_{A2}(s) - (1 + C_5) F_e(s), \tag{31}$$

https://doi.org/10.1017/S026357471400191X Published online by Cambridge University Press

where $V_{A1}(s) = C_3 F_{\mathrm{h}}(s)$, $I_{B1}(s) = C_1 \dot{x}_{\mathrm{m}}(s)$, $I_{A2}(s) = C_4 \dot{x}_{\mathrm{s}}(s)$, $V_{B2}(s) = \mathrm{C}_2 F_e(s)$. Z Substituting (26)–(29) into (30) and (31), the dynamic equations of the overall system can be expressed by (32) and (33):

$$\begin{aligned}&\left[G_m^{-1} + C_m + b_2 \mathrm{C}_1 \left(1 - e^{-s(T_1+T_2)}\right)\right] \dot{x}_m(s) \\ &\quad = -\mathrm{C}_4 e^{-sT_2} \dot{x}_s(s) + (1 + C_6 - b_1 \mathrm{C}_3) F_h(s) - \mathrm{C}_2 e^{-sT_2} F_e(s), \end{aligned} \tag{32}$$

$$\begin{aligned}&\left[G_{\mathrm{s}}^{-1} + C_{\mathrm{s}} + \frac{C_4}{b_1}(1 - e^{-s(T_1+T_2)})\right] \dot{x}_{\mathrm{s}}(s) \\ &\quad = C_1 e^{-sT_1} \dot{x}_{\mathrm{m}}(s) + C_3 e^{-sT_1} F_{\mathrm{h}}(s) - \left(\frac{C_2}{b_2} + 1 + C_5\right) F_e(s). \end{aligned} \tag{33}$$

3.2. Transparency analysis and controller parameter setting

A teleoperation system is defined as transparent if the human operator has an accurate perception of the remote environment and can easily perform the remote task. System transparency can be illustrated by the hybrid matrix $H(s)$ of a bilateral teleoperation system given in (34).

$$\begin{bmatrix} F_{\mathrm{h}}(s) \\ -\dot{x}_{\mathrm{s}}(s) \end{bmatrix} = \begin{bmatrix} H_{11}(s) & H_{12}(s) \\ H_{21}(s) & H_{22}(s) \end{bmatrix} \begin{bmatrix} \dot{x}_{\mathrm{m}}(s) \\ F_e(s) \end{bmatrix} = H(s). \tag{34}$$

Based on (34), hybrid matrix $H(s)$ is defined by ref. [25], which can be interpreted as

$$\mathrm{H}(s) = \begin{bmatrix} H_{11}(s) & H_{12}(s) \\ H_{21}(s) & H_{22}(s) \end{bmatrix} = \begin{bmatrix} Z_{\mathrm{h}} & \text{Force scaling} \\ \text{Velocity scaling} & Z_e^{-1} \end{bmatrix}.$$

The hybrid parameters $h_{ij}, i, j = 1, 2$, are functions of the master/slave dynamics and the control parameters. The main effect of $H(s)$ is to present kinesthetic feedback between the human operator and the environment, and build a relationship between force and velocity. $H_{11}(s)$ and $H_{22}(s)$ denote the operator impedance and environment admittance. Under condition of ideal transparency, the technical medium between the operator and the environment is not felt. That is, Z_{h} and Z_e^{-1} are equal to zero. H_{12} and H_{21} represent the measure of force scaling and velocity scaling, respectively. In order to achieve the ideal transparency in a bilateral teleoperation system in the presence of time delay, the delayed kinematic correspondence and the delayed interaction force correspondence are expressed as $\dot{x}_{\mathrm{s}}(s) = \dot{x}_{\mathrm{m}}(s) e^{-sT}$ and $F_{\mathrm{h}}(s) = F_e(s) e^{-sT}$, respectively. Accordingly, the hybrid matrix in the time-delay-based ideal transparency is expressed as

$$H_{\mathrm{ideal}}(s) = \begin{bmatrix} 0 & e^{Ts} \\ e^{-Ts} & 0 \end{bmatrix}. \tag{35}$$

After transformation, the dynamic Eqs. (32) and (33) of the overall system can be expressed by (34) to demonstrate the transparency of the proposed system. The parameters of the hybrid matrix $H(s)$ are shown in (36)–(40) where Den denotes the denominator of each term:

$$H_{11} = \left[G_{\mathrm{m}}^{-1} + C_{\mathrm{m}} + b_2 C_1 \left(1 - e^{-s(T_1+T_2)}\right)\right] \left[G_{\mathrm{s}}^{-1} + C_{\mathrm{s}} + \frac{C_4}{b_1} \left(1 - e^{-s(T_1+T_2)}\right)\right] + C_4 C_1 e^{-s(T_1+T_2)}, \tag{36}$$

$$H_{12} = -C_4 e^{-sT_2} \left(\frac{C_2}{b_2} + 1 + C_5\right) + C_2 e^{-sT_2} \left[G_{\mathrm{s}}^{-1} + C_{\mathrm{s}} + \frac{C_4}{b_1} \left(1 - e^{-s(T_1+T_2)}\right)\right], \tag{37}$$

$$H_{21} = -\left(1 + C_6 - b_1 C_3\right) C_1 e^{-sT_1} - C_3 e^{-sT_1} \left[G_{\mathrm{m}}^{-1} + C_{\mathrm{m}} + b_2 C_1 \left(1 - e^{-s(T_1+T_2)}\right)\right], \tag{38}$$

https://doi.org/10.1017/S026357471400191X Published online by Cambridge University Press

$$H_{22} = -C_2C_3e^{-s(T_1+T_2)} + \left(\frac{C_2}{b_2} + 1 + C_5\right)(1 + C_6 - b_1C_3)\,, \tag{39}$$

$$\text{Den} = -C_4C_3e^{-s(T_1+T_2)} + (1 + C_6 - b_1C_3)\left[G_s^{-1} + C_s + \frac{C_4}{b_1}(1 - e^{-s(T_1+T_2)})\right]. \tag{40}$$

According to (34), to achieve high transparency, the operator impedance and environmental admittance should be close to zero. To achieve highly accurate force and trajectory tracking in the presence of time delays, the force scaling and velocity scaling should be e^{sT} and e^{-sT}, respectively. Under constant time delay or slow time varying delay conditions, the characteristic of the time delay element e^{-sT} in the frequency domain is described as:

$$\left|e^{-sT}\right| = 1. \tag{41}$$

Accordingly, based on (36) and (41), $|H_{11}| = \left|(G_m^{-1} + C_m)(G_s^{-1} + C_s) + C_4C_1e^{-s(T_1+T_2)}\right|$. Therefore, by setting the velocity controllers C_4 and C_1 as (42) and (43), the operator impedance H_{11} is close to 0.

$$C_1 = G_m^{-1} + C_m, \tag{42}$$

$$C_4 = -G_s^{-1} - C_s, \tag{43}$$

where the velocity controller C_m and C_s are defined as $C_{m,s} = \frac{1}{s}k_p + k_v$. k_p and k_v are the position and velocity control gains, respectively. Hence, C_1 and C_4 are defined as: $C_1 = \frac{1}{s}k_p + k_v + m_ms$, $C_4 = \frac{1}{s}k_p + k_v + m_ss$, respectively. Accordingly, the controllers C_1 and C_4 allow position information transmission which will enhance the trajectory tracking performance of the proposed 4-CH system.

Based on (39) and (41), the environmental admittance H_{22} is close to zero as shown in the following equation:

$$C_3 = 1 + C_6 - b_1C_3, \tag{44}$$

$$C_2 = \frac{C_2}{b_2} + 1 + C_5. \tag{45}$$

Substituting (37), (41), (43), (44), and (45) into (37) and (40), the force scaling H_{12}/Den can be simplified as $\frac{H_{12}}{\text{Den}} = \frac{C_2}{C_3}e^{sT_1}$. Therefore, highly accurate force tracking can be achieved via the following setting:

$$C_2 = C_3. \tag{46}$$

Normally, the force signal transmission controllers C_2 and C_3 are designed as: $C_2 = C_3 = 1$. Therefore, (44) and (45) can be simplified as:

$$C_6 = b_1, \tag{47}$$

$$C_5 = -\frac{1}{b_2}. \tag{48}$$

Substituting (41)–(48) into (38), the velocity scaling H_{21}/Den can be simplified as $\frac{H_{21}}{\text{Den}} = e^{-sT_1}$. Hence, position drift, which is the main drawback of the modified wave transformation controllers, can be reduced and accurate trajectory tracking is achieved.

Through setting the controller parameters to satisfy (42)–(48), high transparency in the proposed architecture can be achieved in the presence of time delays.

https://doi.org/10.1017/S026357471400191X Published online by Cambridge University Press

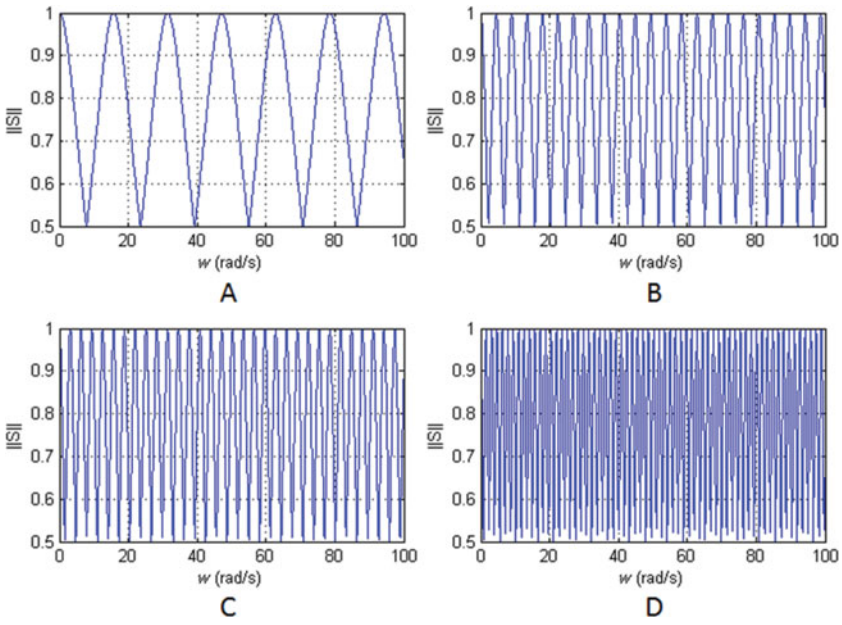

Fig. 5. Scattering norm of the modified wave transformation controller 1 with different time delays: A. 200 ms, B. 700 ms, C. 1000 ms, D. 2000 ms.

3.3. Stability analysis

This section analyzes the stability performance of the proposed 4-CH architecture in order to prove that this approach is able to achieve high transparency without sacrificing system stability. Based on (26)–(29), the two modified wave transformation controllers can be expressed in the form of the following hybrid matrices:

$$\begin{bmatrix} V_{A1}(s) \\ -I_{A2}(s) \end{bmatrix} = \begin{bmatrix} H_{11}(s) & H_{12}(s) \\ H_{21}(s) & H_{22}(s) \end{bmatrix} \begin{bmatrix} I_{A1}(s) \\ V_{A2}(s) \end{bmatrix} = \begin{bmatrix} \frac{1}{b_1}\left[1 - e^{-s(T_1+T_2)}\right] & e^{-sT_2} \\ -e^{-sT_1} & b_1 \end{bmatrix} \begin{bmatrix} I_{A1}(s) \\ V_{A2}(s) \end{bmatrix}, \quad (49)$$

$$\begin{bmatrix} V_{B1}(s) \\ -I_{B2}(s) \end{bmatrix} = \begin{bmatrix} H_{11}(s) & H_{12}(s) \\ H_{21}(s) & H_{22}(s) \end{bmatrix} \begin{bmatrix} I_{B1}(s) \\ V_{B2}(s) \end{bmatrix} = \begin{bmatrix} b_2\left[1 - e^{-s(T_1+T_2)}\right] & e^{-sT_2} \\ -e^{-sT_1} & \frac{1}{b_2} \end{bmatrix} \begin{bmatrix} I_{B1}(s) \\ V_{B2}(s) \end{bmatrix}. \quad (50)$$

Anderson and Spong[3] state that a teleoperation system is passive, if and only if the norm of the scattering matrix $S(s)$ is equal to or less than one, where $S(s)$ is expressed as

$$S(s) = \begin{bmatrix} 1 & 0 \\ 0 & -1 \end{bmatrix} [H(s) - I][H(s) + I]^{-1}. \quad (51)$$

Based on (51), the scattering norm S is influenced by the angular frequency ω ($s = j\omega$) of the time delay component $e^{-sT_{1,2}}$. The periodicity of $e^{-sT_{1,2}}$ indicates that the scattering norm S is periodic. Since the angular frequency can be considered as a factor of the product of $\omega T_{1,2}$, different time delays $T_{1,2}$ can be treated as the gains of the angular frequency to influence the scattering norm by which the scattering norm S can be extended or compressed periodically. Accordingly, Figs. 5 and 6 display the values of the scattering norm S with ω changing. As shown in Figs. 5 and 6, by setting the characteristic impedance b_1 and b_2 as positive constants, the values of time delays only influence changes in the frequency of the waveform rather than the magnitude of the scattering norm. The vertex of the scattering norm remains unchanged. Accordingly, the scattering norm S of the proposed scheme is uniformly no more than 1. Therefore, the passivity and stability of the communication channels in the proposed 4-CH architecture can be guaranteed.

Assuming the impedances of human operator and environment are passive[15] has already proved that the modal spaces of master and slave are stable in the usual cases when the passivity of the

https://doi.org/10.1017/S026357471400191X Published online by Cambridge University Press

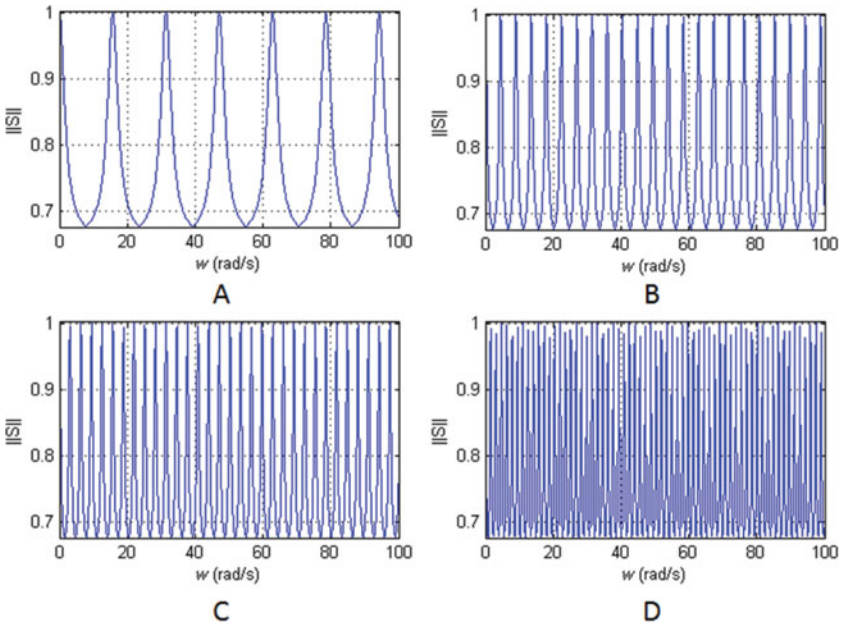

Fig. 6. Scattering norm of the modified wave transformation controller 2 with different time delays: A. 200 ms, B. 700 ms, C. 1000 ms, D. 2000 ms.

delay-based communication channels is guaranteed. In order to further improve the stability on the master side and the slave side, the velocity damping approach can be alternatively applied, since velocity damping by local velocity feedback is able to enhance the stability of each modal space.[26] However, setting a velocity damping controller as a constant value can also degrade the system transparency. The instability of the delay-based control system is caused by the time delay element e^{-sT} in the high-frequency area.[7] In order to eliminate high-frequency perturbations on both the master and slave sides without sacrificing system transparency, the velocity damping controller is designed to be a high-pass filter rather than a constant gain. The local velocity feedback controllers C_{m} and C_{s} can be rewritten as

$$C_{\mathrm{m,s}} = \frac{1}{s}k_{\mathrm{p}} + k_{\mathrm{v}} + \frac{s^2}{(s+p)^2}, \tag{52}$$

where p is the cut-off frequency of the high-pass filter. The reason for choosing a second-order high-pass filter is that its bandwidth is better than that of the first-order high-pass filter.[27] By applying high-pass filters, the high-frequency vibrations in force and trajectory tracking in the transient state can be mitigated even in the presence of a large time delay.

4. Experiment Results

Figure 7 shows the experimental platform which is a bilateral teleoperation set up for the study of the proposed algorithms. The HILINK microcontroller board[28] is interfaced with a computer to control a set of DC motors on both the master and the slave sides. The control algorithms are developed in Matlab/Simulink and downloaded to HLINK boards. The communication channel between the master computers and the slave computers is the Internet. In order to test the proposed system's work performance under larger time delays, the time delay blocks in the Simulink library are applied to the algorithms of the two computers. The one-way time delay of these experiments is approximately 200 ms (400 ms round trip time); comparable to the round trip transit time of an Internet User Datagram Packet from Australia to the US.[29]

The four DC motors in Fig. 7 represent the operator motor, the master motor, the slave motor, and the environmental load motor. On the master side, the operator motor and the master motor are coupled mechanically so that the operator motor can act like the human operator to physically

https://doi.org/10.1017/S026357471400191X Published online by Cambridge University Press

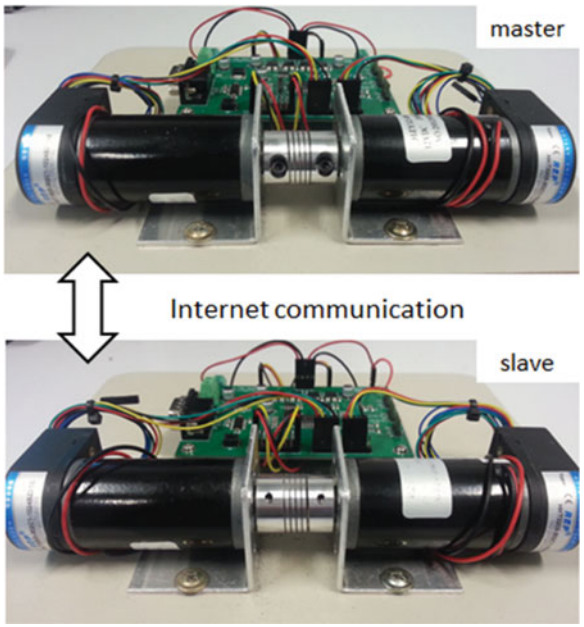

Fig. 7. Experiment setup.

control the master motor. Then, the Hilink board derives the velocity and force command signals generated from the master motor, and then the signals are transmitted to the computer on the slave side via the Internet. On the slave side, the slave motor and the environmental load motor are also mechanically coupled. The slave motor receives the velocity and force command signals and then moves accordingly. The environmental load motor can apply different environmental contact loads to the slave motor. Matlab/Simulink/Real-Time Workshop is the software applied for controlling the motors.

In the proposed control system, the sampling period is 0.1 ms. The two wave characteristic impedances b_1 and b_2 are set as 2.5 Ns/m. Position gain k_p and velocity control gains k_v are set as 4.7 N/m and 2.3 Ns/m, respectively. The value of the constant force control gains C_2, C_3, C_5, and C_6 are 1, 1, −0.4, and 2.5, respectively. The parameter p of the high-pass filter is 1.

In order to test the performance of the proposed 4-CH architecture in enhancing transparency, the force tracking, velocity tracking, and position tracking of the proposed four-channel system are compared against the two systems proposed in previous work, the 4-CH architecture applying wave transform controllers in Fig. 3[15] (system A) and the 2-CH reducing wave-variable-based reflection teleoperation system in ref. [21] (system B). The experiments are conducted for three scenarios: free space motion, hard contact with the environment, and high-frequency contact with the environment. All gain values for the controllers and dynamics remain unchanged throughout the experiments.

4.1. Free motion

In this experiment, to represent free space movement, a square signal at a frequency of 0.5 rad/s is applied to the motor representing the operator and zero input into the motor representing the environment. The performance of systems *A* and *B* and our proposed 4-CH system in free motion are shown in Figs. 8, 9, and 10, respectively. In Fig. 8, the value of the low-pass filters located in the communication channels of the system must be set at a small value in order to reduce the oscillations caused by the time delays and wave reflections. However, in the presence of large time delays, the delay-based bias term $\left[(b + bC_6 - C_3)\, F_h \times e^{-sT} W - (bC_2 - 1 - C_5)\, F_e\right]$ in (20) causes signal variations and adversely influences the accuracy of trajectory tracking as shown in Figs. 8B and 8C. As shown in Figs. 9B and 9C, accurate trajectory tracking can be achieved since the wave-variable-based reflections are reduced in system *B*. However, since the master motor has a velocity during free motion, the bias term $b\dot{x}_m(s)$ in (15) adversely affects the force feedback so that the force signals in Fig. 9A vary widely. In Fig. 10, the oscillations caused by wave-variable-based reflections are

https://doi.org/10.1017/S026357471400191X Published online by Cambridge University Press

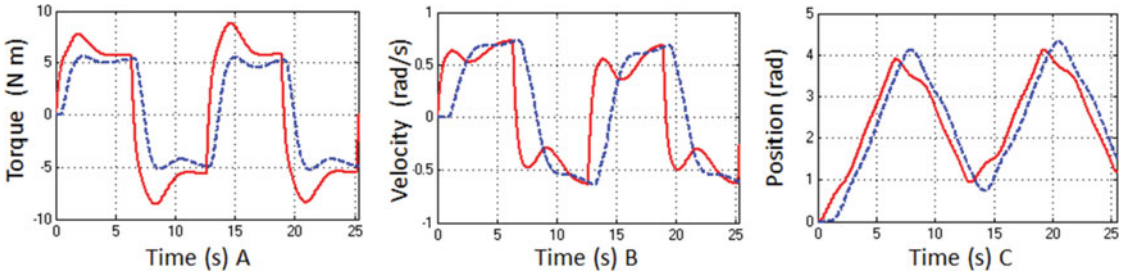

Fig. 8. Free motion of system *A*: A. Force tracking of master and slave motors, B. Velocity tracking of the master and slave motors, C. Position tracking of the master and slave motors (red curved—master, blue dotted—slave).

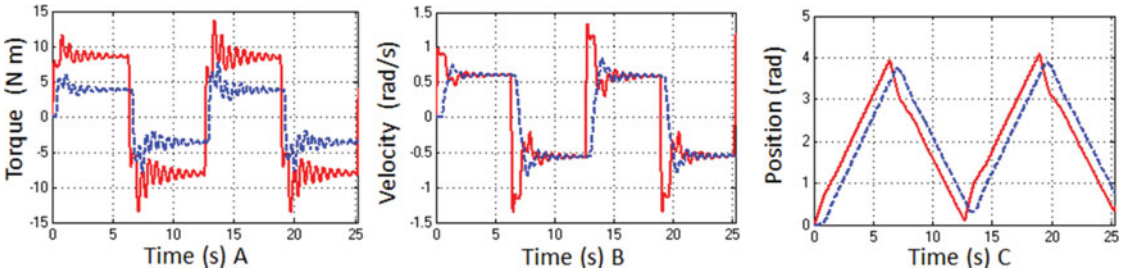

Fig. 9. Free motion of system *B*: A. Force tracking of master and slave motors, B. Velocity tracking of the master and slave motors, C. Position tracking of the master and slave motors (red curved—master, blue dotted—slave).

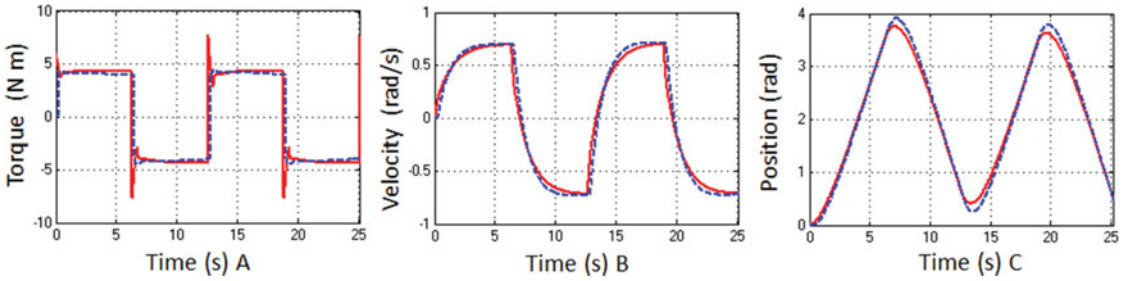

Fig. 10. Free motion of the proposed 4-CH system: A. Force tracking of master and slave motors, B. Velocity tracking of the master and slave motors, C. Position tracking of the master and slave motors (red curved—master, blue dotted—slave).

eliminated as shown in Fig. 10A and highly accurate trajectory tracking is achieved in the proposed 4-CH architecture as shown in Figs. 10B and 10C.

4.2. Hard environmental contact

During the hard contact with the environment, a square signal command with 0.5 rad/s frequency is applied to the motor representing the operator, and an opposite square signal command with the same magnitude and frequency is applied to the environment motor. Figs. 11, 12, and 13 illustrate the performances of systems *A* and *B* and our proposed 4-CH system in hard contact with the environment, respectively

As shown in Fig. 11, the applied extra control parameters of the extended Laurence architecture enable the accurate force tracking performance in system *A*. However, since the wave-based reflections still exist, the force tracking still has small variations even when wave filtering is applied, as shown in Fig. 11A. The trajectory tracking is adversely affected by the bias terms of the applied conventional wave transformation controllers, as shown in Figs. 11B and 11C so that position drift occurs. In Fig. 12, during steady-state contact with the environment, the velocities of the master and slave motors are zero. Therefore, the bias term $b\dot{x}_{\mathrm{m}}(s)$ in (15) acts as a damping element to guarantee the accurate force tracking of system *B*. However, the bias term also leads to large position drift as shown

https://doi.org/10.1017/S026357471400191X Published online by Cambridge University Press

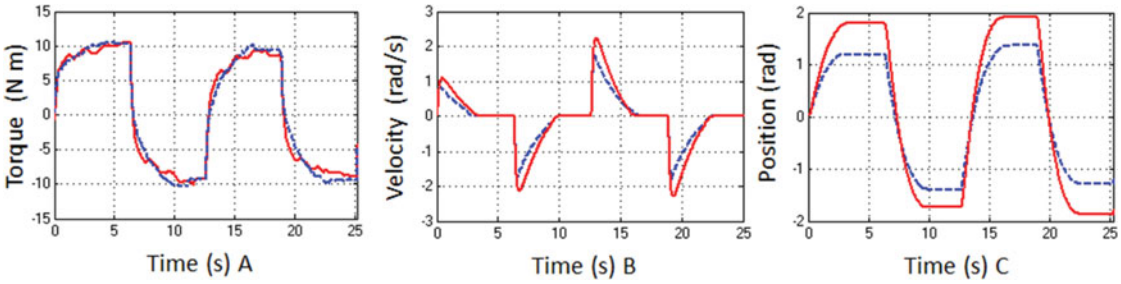

Fig. 11. Hard environmental contact of system *A*: A. Force tracking of master and slave motors, B. Velocity tracking of the master and slave motors, C. Position tracking of the master and slave motors (red curved—master, blue dotted—slave).

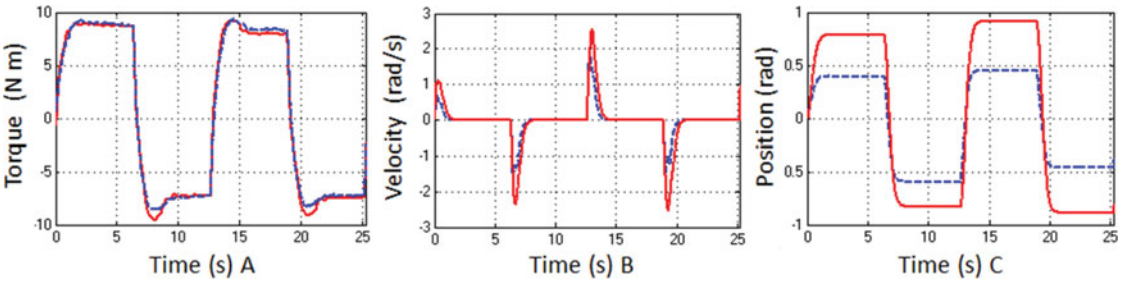

Fig. 12. Hard environmental contact of system *B*: A. Force tracking of master and slave motors, B. Velocity tracking of the master and slave motors, C. Position tracking of the master and slave motors (red curved—master, blue dotted—slave).

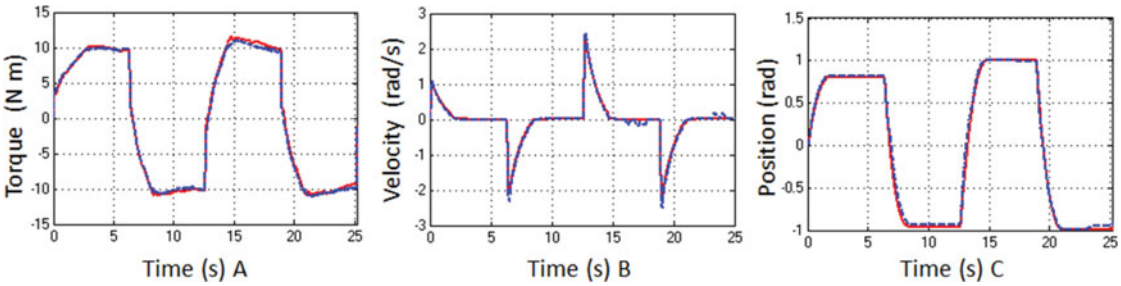

Fig. 13. Hard environmental contact of the proposed 4-CH system: A. Force tracking of master and slave motors, B. Velocity tracking of the master and slave motors, C. Position tracking of the master and slave motors (red curved—master, blue dotted—slave).

in Fig. 12C. Compared with these two systems, since the wave-based reflections are reduced and the bias terms of the modified wave transformation controllers are compensated for by the controllers on the master side and the slave side, both the trajectory tracking and force tracking of the proposed 4-CH system have better performance, as shown in Fig. 13.

4.3. High-frequency environmental contact

High-frequency haptic feedback, which provides information about macroscopic material properties and precise surface features, is particularly useful for teleoperation systems. Without high-frequency haptic feedback, all remote objects manipulated by the human operator are perceived as soft with a smooth surface. Therefore, high-frequency environmental contact is also a significant criterion for testing the performance of a system. In this experiment, the human operator motor applies a constant force to the master, and at the same time, the environment motor applies an opposite force with high-frequency vibration to the slave.

As shown in Fig. 14, due to limited bandwidth, the high-frequency force signals from the environment are seriously degraded by the low pass filters in the communication channels as shown in Fig. 14B. Figure 15 illustrates the performance of system B. Since high-frequency signal causes

https://doi.org/10.1017/S026357471400191X Published online by Cambridge University Press

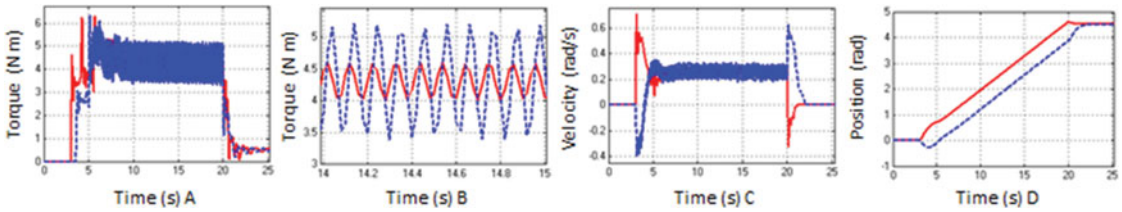

Fig. 14. High-frequency environmental contact of system *A*: A. Force tracking of master and slave motors, B. Magnified drawing of the force signals, C. Velocity tracking of the master and slave motors, D. Position tracking of the master and slave motors (red curved—master, blue dotted—slave).

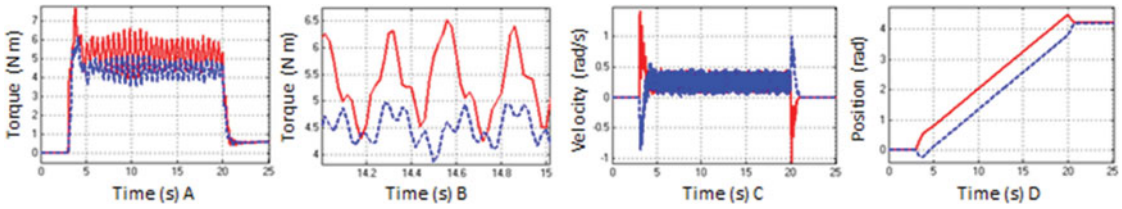

Fig. 15. High-frequency environmental contact of system *B*: A. Force tracking of master and slave motors, B. Magnified drawing of the force signals, C. Velocity tracking of the master and slave motors, D. Position tracking of the master and slave motors (red curved—master, blue dotted—slave).

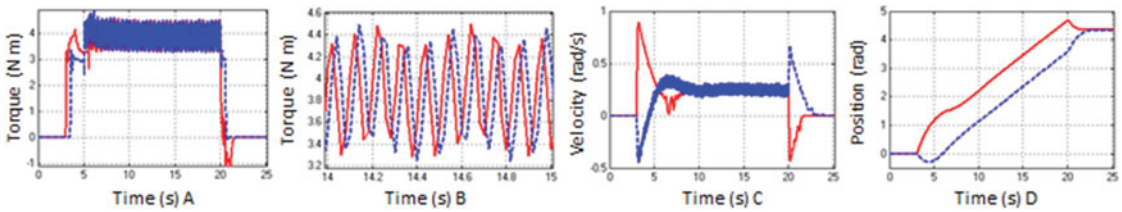

Fig. 16. High-frequency environmental contact of the proposed 4-CH architecture: A. Force tracking of master and slave motors, B. Magnified drawing of the force signals, C. Velocity tracking of the master and slave motors, D. Position tracking of the master and slave motors (red curved—master, blue dotted—slave).

vibration in the whole system, there is large variation in the velocities of the three systems (Figs. 14C, 15C, and 16C). Accordingly, the bias term $b\dot{x}_{\mathrm{m}}(s)$ in (15) enlarges and distorts the master force signals of system *B* as shown in Figs. 15A and 15B. Compared with these two systems, without using wave filtering, the proposed system has a satisfactory high-frequency information transmission ability since accurate high-frequency force tracking is achieved without distortion, magnification, or degradation as shown in Figs. 16A and 16B. Figs. 16C and 16D illustrate that in spite of transmitting high-frequency signals, the trajectory tracking performance of the proposed 4-CH system is not adversely affected by the high-frequency perturbation.

The experimental results strongly confirm the effectiveness of the proposed 4-CH system in achieving an optimal trade-off between stability and transparency by reducing wave-variable-based reflections. The experiment results for different environment situations (free space movement, hard environmental contact and high-frequency environmental contact) also illustrate that, compared with systems *A* and *B*, the proposed 4-CH system has superior performance in complex, unknown environment.

5. Conclusion

In this paper, an innovative 4-CH system with two modified wave transformation controllers for reducing wave-based reflections is proposed to achieve high delay-based transparency and simultaneously guarantee system stability in the presence of time delays. The delay-based stability and conditions for realizing high transparency are analyzed in this paper. The experimental results for different environmental situations confirm that the proposed system can achieve performance which

https://doi.org/10.1017/S026357471400191X Published online by Cambridge University Press

is superior to previous work in achieving the optimal trade-off between transparency and stability in the presence of large time delays.

References

1. C. Passenbarg, A. Peer and M. Buss, "A survey of environment-, operator-, and task-adapted controllers for teleoperation systems," *Mechatronics* **20**, 787–801 (Oct. 2010).
2. D. A. Lawrence, "Towards Force Reflecting Teleoperation Over The Internet," *Proceedings of the IEEE International Conference on Robotics and Automation*, Nice, France (May 12–14, 1992), vol. 2, pp. 1406–1411.
3. R. J. Anderson and M. W. Spong, "Bilateral control of teleoperators with time delay," *IEEE Trans. Autom. Control* **34**(5), 494–501 (May 1989).
4. G. Niemeyer and J. J. E. Slotine, "Stable adaptive teleoperation," *IEEE J. Ocean. Eng.* **16**(1), 152–162 (1991).
5. D. A. Lawrence, "Stability and transparency in bilateral teleoperation," *IEEE Trans. Robot. Autom.* **9**(5), 624–637 (1993).
6. B. Zhang, K. Alexandre and J.-P. Richard, "H∞ Control of Delayed Teleoperation Systems Under Polytopic-Type Uncertainties," *Proceedings of the 20th Mediterranean Conference on Control & Automation (MED)*, Barcelona, Spain (Jul. 3–6, 2012) pp. 954–959.
7. M. Franke, S. Stramigioli, S. Misra, C. Secchi and A. Macchelli, "Bilateral telemanipulation with time delays: A two-layer approach combining passivity and transparency," *IEEE Trans. Robot.* **27**(4), 741–756 (2011).
8. Y. Yokokohji, T. Imaida and T. Yoshikawa, "Bilateral Teleoperation Under Time-Varying Communication Delay," *Proceedings of the IEEE/RSJ International Conference on Intelligent Robots and Systems*, Kyongju, South Korea (Oct. 17–21, 1999), vol. 3, pp. 1854–1859.
9. Y. Yokokohji, T. Imaida and T. Yoshikawa, "Bilateral Control with Energy Balance Monitoring Under Time-Varying Communication Delay," *Proceedings of the IEEE International Conference on Robotics and Automation*, San Francisco, USA (Apr. 24–28, 2000), vol. 3, pp. 2684–2689.
10. S. Munir and W. J. Book, "Wave-Based Teleoperation with Prediction," *Proceedings of the American Control Conference*, Arlington, USA (Jun. 25–27, 2001) pp. 4605–4611.
11. S. Munir and W. J. Book, "Internet-based teleoperation using wave-variables with prediction," *IEEE/ASME Trans. Mechatronics*, **7**(2), 124–133 (2002).
12. Y. Ye and P. Liu, "Improving haptic feedback fidelity in wave-variable-based teleoperation orientated telemedical applications," *IEEE Trans. Instrum. Meas.* **58**(8), 2847–2855 (2009).
13. Y. Ye and P. X. Liu, "Improving trajectory tracking in wavevariable- based teleoperation," *IEEE/ASME Trans. Mechatronics* **15**(2), 321–326 (2010).
14. D. Tian, D. Yashiro and K. Ohnishi, "Frequency-Domain Analysis of Wave Variable Based Teleoperation and its Equivalent Implementation," *Proceedings of the 1st International Symposium on Access Space*, Yokohama, Japan (Jun. 17–19, 2011) pp. 41–46.
15. A. Aziminejad, M. Tavakoli, R. V. Patel and M. Moallem, "Transparent time delayed bilateral teleoperation using wave variables," *IEEE Trans. Control Syst. Technol.* **16**(3), 548–555 (May 2008).
16. B. Yalcin and K. Ohnishi, "Stable and transparent time-delayed teleoperation by direct acceleration waves," *IEEE Trans. Ind. Electron.* **57**(9), 3228–3238 (Sep. 2010).
17. G. Niemeyer and J. Slotine, "Transient Shaping in Force-Reflecting Teleoperation," *Proceedings of the 5th International Conference on Advanced Robotics*, Pisa Italy (Jun. 19–22, 1991), vol. 1, pp. 261– 266.
18. G. Niemeyer, Using Wave Variables in Time Delayed Force Reflecting Teleoperation, *Ph.D. Dissertation* (Cambridge, MA: MIT, Sep. 1996).
19. C. Benedetti, M. Franchini and P. Fiorini, "Stable Tracking in Variable Time-Delay Teleoperation," *Proceedings of the IEEE International Conference on Intelligent Robots and Systems*, Maui, USA (Oct. 29–Nov. 3, 2001), vol. 4, pp. 2252–2257.
20. H. Ching, Internet-Based Bilateral Teleoperation, *Ph.D. Dissertation*, (Atlanta, GA: Georgia Institute of Technology, Dec. 2006).
21. L. Bate, C. D. Cook and Z. Li, "Reducing wave-based teleoperator reflections for unknown environments," *IEEE Trans. Ind. Electron.* **58**(2), 392–397 (2011).
22. Y. Yokokohji and T. Yoshikawa, "Bilateral control of master-slave manipulators for ideal kinesthetic coupling-formulation and experiment," *IEEE Trans. Robot. Autom.* **10**(5), 605–619 (1994).
23. K. Hashtrudi-Zaad and S.E. Salcudean, "Transparency in time-delayed systems and the effect of local force feedback for transparent teleoperation," *IEEE Trans. Robot. Autom.* **18**(1), 108–114 (Feb. 2002).
24. E. Naerum and B. Hannaford, "Global Transparency Analysis of the Lawrence Teleoperator Architecture," *Proceedings of the IEEE International Conference on Robotics and Automation*, Kobe, Japan (May 12–17, 2009), pp. 4344–4349.
25. B. Hannaford, "A design framework for teleoperators with kinesthetic feedback," *IEEE Trans. Robot. Autom.* **5**(4), 426–434 (Aug. 1989).
26. A. Suzuki and K. Ohnishi, "A Constitution Method of Bilateral Teleoperation Under Time Delay Based on Stability Analysis of Modal Space," *Proceedings of the IEEE International Symposium on Industrial Electronics*, Bari, Italy (Jul. 4–7, 2010) pp. 2277–2282.

https://doi.org/10.1017/S026357471400191X Published online by Cambridge University Press

27. A. Suzuki and K. Ohnishi, "Novel four-channel bilateral control design for haptic communication under time delay based on modal space analysis," *IEEE Trans. Control Syst. Technol.* **21**(3), 882–890 (May 2013).
28. Zeltom Educational and Industrial Control Systems, http://zeltom.com/products/hilink (last accessed 29 November 2013).
29. L. Bate and C. Cook, "Exploration of Intelligible Force Feedback for Telesurgery over the Internet," *Proceeding of the International Conference on Information Technology in Mechatronics*, Istanbul, Turkey (Oct. 1–6, 2001), pp. 124–129.

https://doi.org/10.1017/S026357471400191X Published online by Cambridge University Press